Conference Paper, Published Version

Antoine, Germain

Tridimensional numerical modelling of the suspended sediment transport dynamic in Loire River

Tridimensional numerical modelling of the suspended sediment transport dynamic in Loire River

Germain ANTOINE
EDF R&D, National Laboratory for Hydraulics and Environment
Saint-Venant Laboratory for Hydraulics
Chatou, France
Email: germain.antoine@edf.fr

***Abstract*—Several studies have been done with the objectives of quantifying and simulating sediment transport and morphodynamics of the Loire River, which is considered as one of the last wild sand bed rivers in Europe. However, few of these studies considered the suspended sediment load dynamics. In this study, a local reach of the Loire River is considered, with a complex geometrical configuration: the river reach is composed with two alternate bars in a bend, an adjacent channel is connected to the river by a lateral weir and the last cross section of the reach is defined by a large step. As the adjacent channel is used for electricity production, the work is focused on the deposition dynamics of suspended sediments coming from the Loire River to this channel.**

A field campaign was performed in 2015 during a flood event, in which measurements were made of both bathymetry and the 3D velocity field with an acoustic Doppler current profiler (aDcp). Based on these field data, a TELEMAC 3D model has been built for simulating flow and suspended sediment dynamics of this site. The hydrodynamic part of the model has been calibrated with the aDcp measurements, and three scenarios of discharge conditions in the Loire River have been defined. In order to represent properly the tridimensional flow patterns measured in the adjacent channel, specific values of wall friction coefficients have been calibrated. For the sediment part of the model, ten grain size classes have been simulated and the deposition patterns and volumes in the channel have been analysed. The comparison between numerical results and grain sizes measurements of deposits in the adjacent channel shows good agreements, and the study highlights the complex interactions and transfers from the Loire River in this configuration.

I. Introduction

Several studies have been done with the objectives of quantifying and simulating sediment transport and morphodynamics of the Loire River ([2], [7], [1]), which is considered as one of the last wild sand bed rivers in Europe. However, few of them considered the suspended sediment load dynamics. Two reasons are mainly reported to explain this lack of suspended sediment study: first the dataset for suspended sediment transport is poor. As the river is wide, with a complex morphology, it is difficult to assess properly suspended sediment fluxes in a river cross section. For the same reasons, the transport of the finer grain sized sediments is complex and could be strongly dominated by tridimensional motions of the flow, which means the use of a qualified 3D model.

In this study, a local reach of the Loire River is considered (Figure 1), with a complex geometrical configuration: the river reach is composed with two alternate bars in a bend, an adjacent channel is connected to the river by a lateral weir and the last cross section of the reach is defined by a large weir. As the adjacent channel is used for electricity production, the work is focused on the deposition dynamics of suspended sediments coming from the Loire River to this channel (Figure 2).

Fig. 1: General overview of the study site

Fig. 2: Deposits observed in the upstream part of the adjacent channel

A field campaign was performed in 2015 during a flood event in order to measure precisely the bathymetry of the river reach and the 3D velocity field using an aDcp. Based on these field data, a TELEMAC 3D model has been built for simulating both hydrodynamics and suspended sediment transport. As the adjacent channel is separated from the Loire River by a step significantly higher than the river bed level, bed load transport has not been considered.

The first part of this paper analyses the data obtained from the field campaign. The second part is about the methodology developed to calibrate the hydrodynamic part of the 3D model, and presents the different scenarios chosen for the numerical simulation. Finally, the third part shows the main results of the hydro-sedimentary model.

II. Field measurements

The field campaign has been performed in moderate flood-discharge conditions in March 2015, during a six-month return period flood. During the campaign, the discharge in Loire River was about 850 m^3/s. Both the bathymetric survey and aDcp measurements were done at the same time and with the same GPS system.

A. Bathymetry

The bathymetry measurements were collected using a multi-beam laser instrument. The bottom of the river reach is presented in Figure 3.

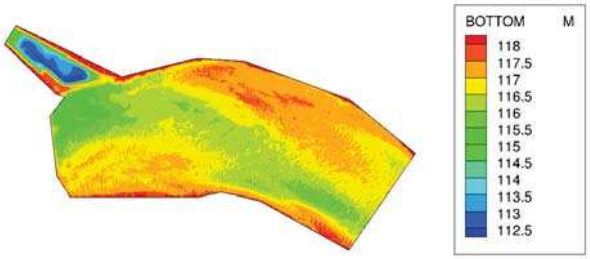

Fig. 3: Bathymetry of the study site

In Figure 3, two large bars can be observed along the reach. The first one, located on the right side, is about 400 meters long and begins at the upstream limit of the study site. The second one, located on the left side, is about 200 meters long and finishes in front of the large weir. On these two bars, it is possible to identify dunes about 70 centimeters high. Between the two bars, a deeper channel makes a straight connection between the left side of the domain entrance and the connection with the adjacent channel. The bottom of the upstream part of the adjacent channel is presented in Figure 4.

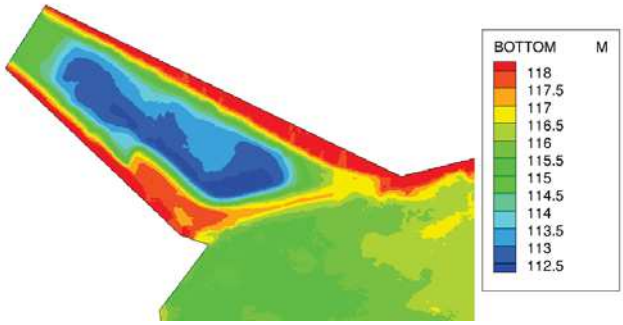

Fig. 4: Bathymetry of the adjacent channel

In the Figure 4, we can notice a significant deposit along the step separating the Loire River and the channel. This deposit propagates towards the downstream part of the channel along the left side. In the centre of the channel, measurements show a large and deep reservoir.

B. Flow velocities

The velocity field of the flow have been measured with a TELEDYN Rio Grande aDcp with a frequency of 600 kHz and with a vertical cell size defined at 25 cm. Along 17 cross profiles in the Loire River and eight profiles in the adjacent channel, five aDcp samples were taken. Along each cross section, these five measurements have been projected and averaged for every vertical and horizontal cells. The depth averaged values of these velocities measured along the profiles in the Loire River are presented in Figure 5, and the ones measured in the adjacent channel in Figure 6.

Fig. 5: Depth averaged velocities measured in the Loire River (in cm/s)

Fig. 6: Depth averaged velocities measured in the adjacent channel (in cm/s)

Figure 5 shows the effect of the complex bathymetry on the spatial distribution of the velocity. On the two bars, the flow velocity decreases with velocities around 1m/s or smaller, and the flow path is concentrated in the main channel between the twos bars. Especially, high velocities have been measured close to the connection with the adjacent channel, with a maximum value of 1.6 m/s.

The velocities measured in the connected channel are significantly smaller than the ones in the Loire river reach (Figure 6). The maximum measured value is about 0.35 m/s, and the aDcp measurement shows a very interesting 2D pattern. Indeed, a double loop of recirculating flow can be observed in this upstream part of the channel. The first loop, close to the river reach connection, rotates clockwise and is two times larger than the second one, counter-clockwise, which is located downstream.

Figure 7 shows a detailed example of spatial distribution of the measured velocities along a cross section in the Loire River, located close to the connection with the adjacent channel. In this figure, it is easy to see the significant magnitude of the transverse and vertical current (black arrows), and the complex distribution of the flow in three dimensions.

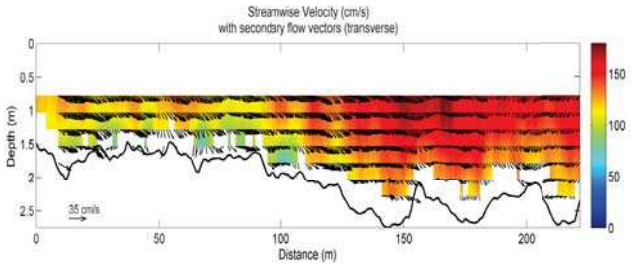

Fig. 7: Local values of flow velocity measured at the P10 cross section

Figure 8 shows another example of measured velocities in a cross section located in the adjacent channel, in the middle of the bigger loop. In this example, we can see that even if the observed velocity magnitudes are almost homogeneous vertically through the water column, the transverse velocities (black arrows) can be significant.

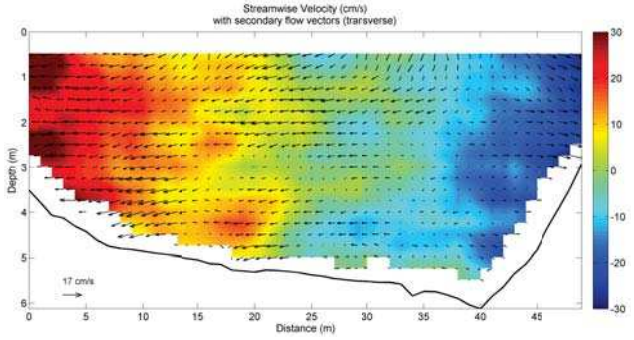

Fig. 8: Local values of flow velocity measured at the P21 cross section

III. Construction of the 3D model and calibration

A. Theoritical background

To simulate hydrodynamics and suspended sediment dynamics for this site, version 7.0 of TELEMAC 3D has been used [4]. The hydraulic part of the model solves a particular case of Navier-Stokes equations [3]. To represent the turbulent processes, several closure equations are available in TELEMAC 3D, as well as for bottom and wall friction source terms.

To simulate the suspended sediment transport dynamic, the hydraulic part of TELEMAC 3D is coupled with the advection dispersion equation, written as follow:

$$\frac{\partial C}{\partial t} + \frac{\partial UC}{\partial x} + \frac{\partial VC}{\partial y} + \frac{\partial}{\partial z}\left(WC - W_s C\right) = \frac{\partial}{\partial x}\left(\nu_t \frac{\partial C}{\partial x}\right) + \frac{\partial}{\partial y}\left(\nu_t \frac{\partial C}{\partial y}\right) + \frac{\partial}{\partial z}\left(\nu_t \frac{\partial C}{\partial z}\right) \quad (1)$$

where C is the suspended sediment concentration, (U, V, W) the three components of the flow velocity, W_s the settling velocity of suspended sediments, and ν_t the turbulent viscosity. The source terms representing the exchanges with the bed (erosion and deposition processes) are calculated as follows:

$$\left(\nu_t \frac{\partial C}{\partial z} + W_s C\right)_{z=Z_b} = F_D - F_E \quad (2)$$

with Z_b the bed level, F_D the deposition flux and F_E the erosion flux.

In this study, we focused on the non-cohesive suspended sediments. With this hypothesis, source terms for erosion and deposition processes are calculated as follow:

$$F_D - F_E = W_s(C_b - C_{eq}) \quad (3)$$

where C_b is the suspended sediment concentration calculated close to the river bed and C_{eq} the equilibrium concentration, calculated with the Zyserman and Fredsoe formula [8].

B. Construction of the 3D model and simulation scenarios

Across the whole domain, a homogeneous irregular mesh was defined, with $\Delta x = 1$ m. On the vertical axis, 10 horizontal plans were defined to discretize the 3D domain (4 128 192 elements).

Three boundary conditions were defined at the liquid boundaries of the domain. The upstream boundary condition is an imposed discharge value and the downstream boundary condition in the Loire River is defined by an imposed value of water level (given by the existing rating curve on the weir). The other downstream boundary condition is located at the end of the adjacent channel, with a imposed discharge value.

For calibrating the hydraulic part of the model, the discharge conditions in Loire $Q_{Measure}$ of the field campaign were chosen. After defining calibration parameters, two other discharge conditions of the Loire River were simulated: the annual mean discharge Q_{Module} and the two years return period flood $Q_{T=2years}$. The Table I shows the BC values for the three discharge conditions.

Scenario	$Q_{upstream}$ Loire (m^3/s)	$Q_{downstream}$ Channel (m^3/s)	$Z_{downstream}$ Loire (m NGF)
$Q_{Measure}$	850	-6.6	118.95
Q_{Module}	328	-6.6	118.11
$Q_{T=2years}$	1600	-6.6	120.02

TABLE I: Definition of the different boundary condition values

For the sediment part of the model, ten sediment classes were simulated separately. As an upstream condition, a fixed suspended sediment concentration of $C_{upstream} = 1$ g/l was defined, with a free fluxes outlet for the downstream boundary conditions. The diameter of these classes (from silt to fine sand) and the associated settling velocity values are presented in Table II.

For these 26 calculation scenarios, the simulation duration was 24 hours of physical time, starting from an initial state

Diameter (μm)	W_s (mm/s)	$Q_{Measure}$	Q_{Module}	$Q_{T=2years}$
40	1.44	C	C	C
63	3.57	C	C	C
100	9.00	C	C	C
150	17.14	C	C	C
200	23.79	C	C	C
300	37.77	C	C	C
400	52.43	C	C	C
600	83.23	C	NC	C
800	115.53	C	NC	C
1200	183.42	NC	NC	C

TABLE II: Sediment parameters for the different simulated scenarios (C: calculated, NC: non-claculated)

with a uniform water level. The steady state for hydraulic was obtained after one and a half hours of physical time. The simulations were performed on the EDF R&D cluster ATHOS, using 96 processors for each run. The spatial distributions of the velocity magnitude, the deposition patterns and volumes into the channel are analysed in the next section.

C. Hydrodynamic calibration

Figure 9 shows the velocity magnitudes simulated at steady state with a Strickler bottom coefficient of $K = 40$ m$^{1/3}$/s. Several values of K were tested, but the value $K = 40$ m$^{1/3}$/s gave the best results. Indeed, we can see that the spatial distribution of the velocities is well correlated to the measured values (Figure 5) : the velocities are smaller on the two alternate bars, and the highest velocities are located in the main bathymetry channel, close to the connection with the adjacent channel. Furthermore, the simulated values are very close to the measured ones.

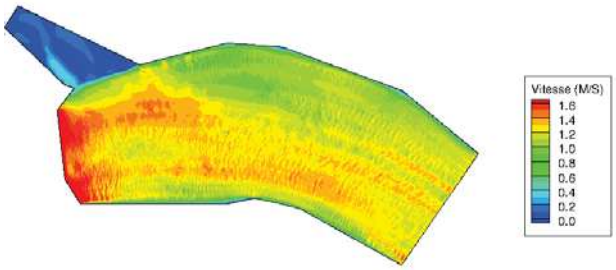

Fig. 9: Simulated depth averaged velocities over the whole domain

The depth averaged velocities were compared to the measured ones along several cross sections. Figure 10 shows an example of results along a river cross section, (total velocity magnitude in red, along X and Y axis components). We can see on this figure that the results are well correlated to the measured ones.

In order to represent properly the flow patterns measured into the adjacent channel, specific values of wall friction coefficients of the Nikuradse law [3] (from $k_{S\ Wall} = 0.01$ to 20 m) and several turbulence models were tested. A 2D geometrical reference of the flow pattern was defined (Figure 11) in order to compare the model output with the measurements. The best agreement was obtained with $k_{S\ Wall} = 5$ m and a $k-\epsilon$ model for both horizontal and vertical dimensions (Figure 12). In this

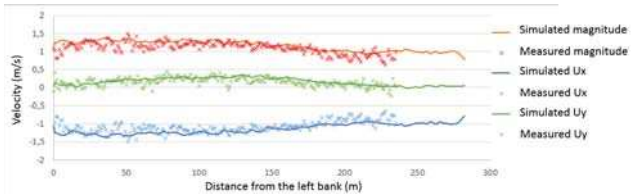

Fig. 10: Example of simulated depth averaged velocities along a cross section (continue lines). Comparison with measurements.

case, the choice of the turbulence model had a smaller effect on the simulation results than the $k_{S\ Wall}$ coefficient. A value of $k_{S\ Wall} = 5$ m could be considered as a non-physical value. However, Patzwahl et Güngör (2015) [6] used a similar values on the Elbe River ($k_{S\ Wall} = 7$ m), justifying this choice by the presence of sheet piling, not represented explicitly in the model.

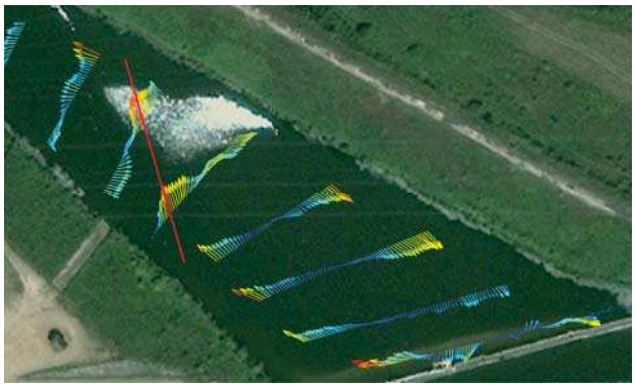

Fig. 11: Geometrical reference (red line)

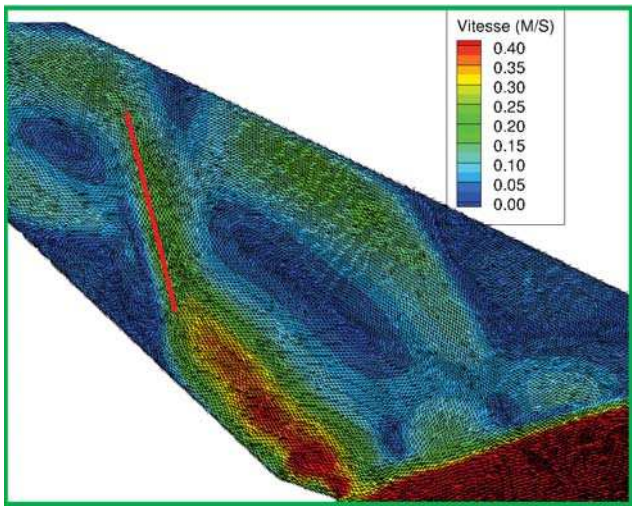

Fig. 12: Calibrated numerical results

IV. RESULTS

A. Flow velocity in the adjacent channel

Depending on the discharge value in the Loire River reach, the flow pattern in the adjacent channel may significantly change. Figure 13 presents the spatial distribution of the calculated velocity magnitudes in the adjacent channel. In this figure, the flow patterns appear to be strongly affected by the changes in discharge conditions in the Loire River. For a discharge value $Q_{T=2years}$ in the Loire River, the double-recirculation pattern is accentuated, with higher velocity magnitudes along the pattern. In this case, the transfer between the river and the channel is accelerated. For Q_{Module}, the velocity magnitudes in the channel decrease and the transferred discharge is not high enough to keep producing the double-recirculation pattern: the simulated results show one small recirculation pattern at the entrance of the channel, with a significant part of the flow rate directed toward the downstream boundary condition.

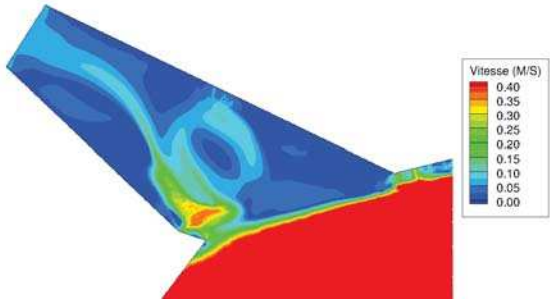

(a) Q_{Module}

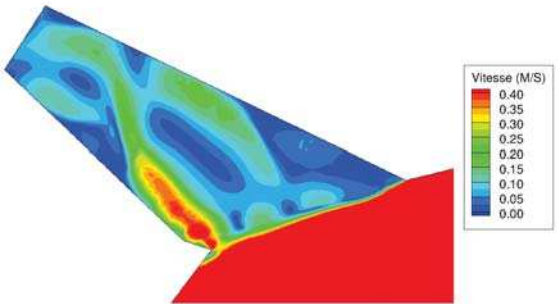

(b) $Q_{Measure}$

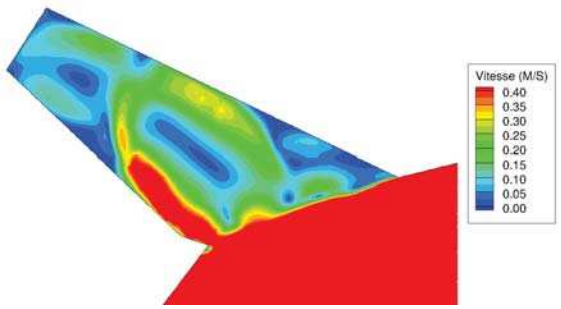

(c) $Q_{T=2years}$

Fig. 13: Simulated velocity magnitude in the adjacent channel for three discharge values in the Loire River

B. Suspended sediment concentration

As the top level of the step separating the adjacent channel from the Loire River is significantly higher than the Loire river bed, the spatial distribution of the suspended sediment concentration in the Loire River reach is of greatest importance for evaluating the sediment transfer to the channel. Depending on the settling velocity of the sediment class and the velocity magnitude in the Loire River, the suspended sediments may be transferred to the adjacent channel over the step.

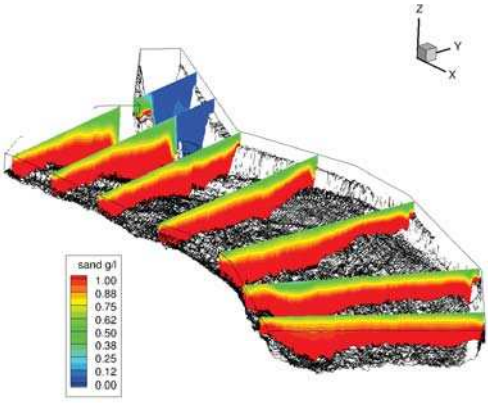

(a) $D = 100$ μm

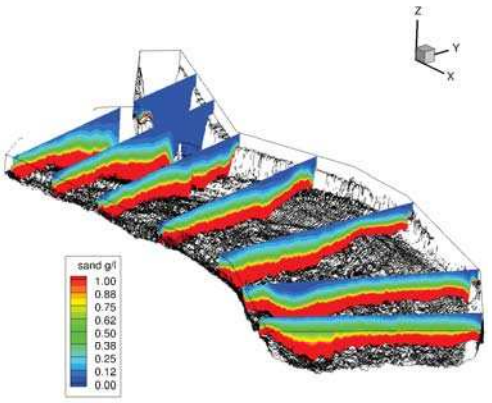

(b) $D = 300$ μm

Fig. 14: Suspended sediment concentration in the Loire River reach for two different sediment classes at $Q_{Measure}$

Figure 14 shows an example of the suspended sediment concentration distribution in the Loire River, in the $Q_{Measure}$ discharge condition and for the sediment classes $D = 100$ μm and $D = 300$ μm. These two figures show clearly that for one given discharge condition, the increase in settling velocity induces a decrease in the suspended sediment concentration transfer to the adjacent channel. For $D = 100$ μm, the suspended sediment concentration is well distributed in the cross sections of the Loire River and is transferred over the top of the adjacent step to the channel. For $D = 300$ μm, the suspended concentration increases with the water depth in any given cross section, so that only a fraction of the sediment fluxes is transferred to the channel.

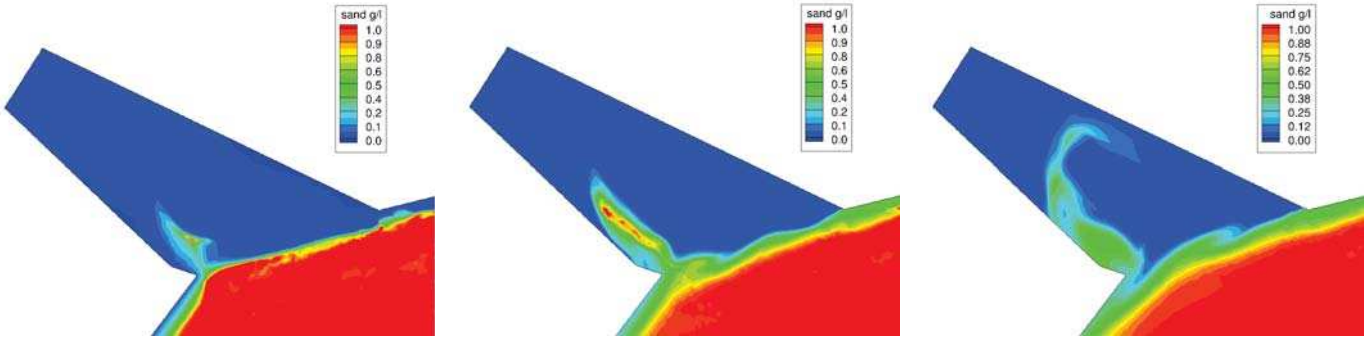

(a) Q_{Module} (b) $Q_{Measure}$ (c) $Q_{T=2years}$

Fig. 15: Spatial distribution of the depth averaged suspended sediment concentration in the adjacent channel for $D = 150$ μm

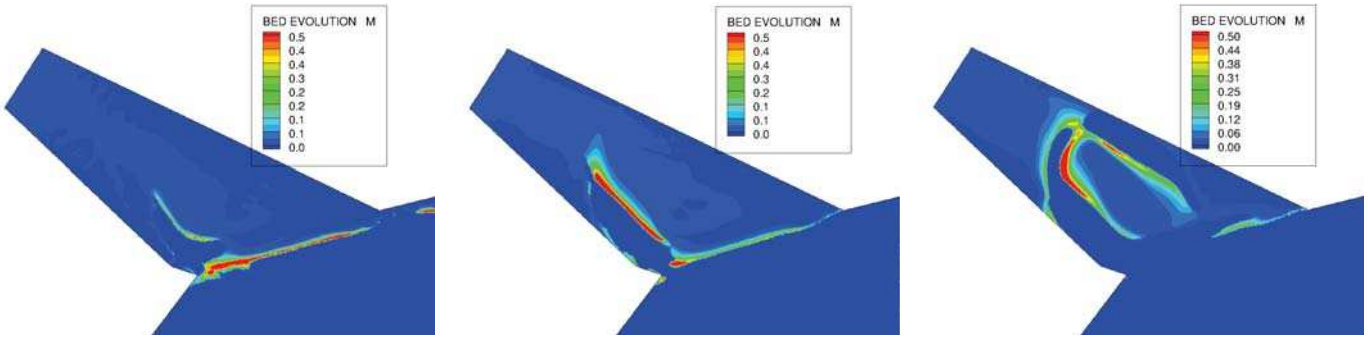

(a) Q_{Module} (b) $Q_{Measure}$ (c) $Q_{T=2years}$

Fig. 16: Spatial distribution of bed evolution in the adjacent channel for $D = 150$ μm at the end of the simulation

The Figure 15 shows the spatial distribution of depth averaged suspended sediment concentration in the adjacent channel, for $D = 150$ μm and the three simulated discharge conditions in the Loire River. These results illustrate the effect of the discharge conditions in the Loire River on the transfer of sediment fluxes to the adjacent channel, for a given sediment class. For Q_{Module} and $Q_{Measure}$, the main part of the suspended sediment flux is transported along the deposit on the left side of the channel. For $Q_{T=2years}$, the suspended sediment flux is transported along the double recirculation pattern to the deepest part of the channel, where it becomes diluted and dispersed.

C. Deposition dynamic in the adjacent channel

The rapid decrease of flow velocity in the adjacent channel increases the deposition probability of suspended sediments. Following the flow patterns observed in the channel, deposition will occur with different spatial distributions and volumes. For a given discharge in Loire River, a decrease of the sediment diameter allows the suspended sediments to be transported further to the downstream part of the adjacent channel and finally, to be dispersed and deposited. For a given sediment class, the increase of discharge condition in the Loire River will produce almost the same effect.

The Figure 16 shows the simulated bed evolution in the channel at the end of the simulation time, for the three tested discharge conditions of the Loire River and $D = 150$ μm. For Q_{Module}, deposition is mainly located on the step separating the Loire River and the channel, with a small deposit on the very upstream part of the left bank. With $Q_{Measure}$, the suspended sediments are transported and deposited further along the left bank deposit. At $Q_{T=2years}$ in the Loire River, the same sediment class propagates to the deepest part of the adjacent channel and is deposited in this zone following the flow pattern.

For each simulation, the sediment volume deposited in the adjacent channel at the end of the simulation has been estimated. These values are presented in Figure 17. This figure shows an interesting result: depending on the discharge value in the Loire River, the maximum value of sediment volume deposited in the channel corresponds to different values of sediment diameter.

For $Q_{T=2years}$, the deposited volume is maximal for $D = 150$ μm, instead of $D = 40$ μm for Q_{Module} and $D = 63$ μm for $Q_{Measure}$. This graph shows also that for a given discharge value in the Loire River, the maximal sediment diameter that can be transferred to the adjacent channel varies widely. As an example, sediment classes with diameters higher than $D = 150$ μm are mainly deposited outside of the channel for Q_{Module}. For $Q_{T=2years}$, the sediment class $D = 800$ μm is still transferred in small quantity to the channel.

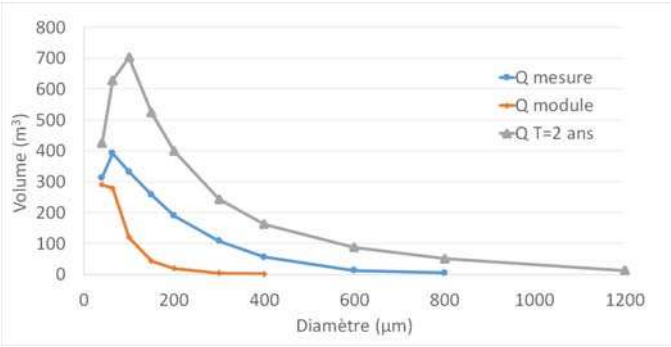

Fig. 17: Deposited volume (in m^3) of sediments in the adjacent channel as a function of sediment diameter

It is important to notice that these results concern absolute values of sediment volumes. However, the total incoming suspended sediment flux is different depending on the discharge condition in Loire River because the upstream suspended sediment concentration has been fixed at $C_{upstream} = 1$ g/l for each scenario. By normalizing the deposited sediment volume with the incoming suspended sediment volume:

$$V_{inlet} = \int_0^{T_{end}} C_{upstream} \times Q_{upstream} \mathrm{d}t \qquad (4)$$

it is possible to better understand the annual deposition dynamic in the channel. Indeed, the highest relative volume of deposited sediment is close to 3%, in the case of Q_{Module} and $D = 40$ μm. For diameters higher than $D = 300$ μm, the relative deposited volume becomes negligible. This results correlates very well with grain size measurements that have been done on deposit samples. These grain size measurements show that the grain size distribution depends on the location in the channel. On the left side deposit, the grain size distribution is mainly centred on one granular mode of $D = 60$ μm. But if we look at the deposits close to the channel step, the grain size distribution is composed with two principal modes: a first one centred on $D = 80$ μm, and a second one on $D = 300$ μm.

Thanks to these measurements and the numerical results, we can build a conceptual scenario of deposition dynamics during a period with successive hydrological events:

- during the usual discharge period, fine sediments ($D < 100$ μm) are transferred and dispersed to the adjacent channel. These fine sediments may come from upper sub-catchments, because for example of a local rain event or upstream dam operations;
- during floods, coarser sediments ($100 < D < 400$ μm) eroded from the sand-river bed are transported by suspension and deposited in the upstream part of the adjacent channel.

V. Discussion

Two points of this work have to be discussed. The first one is about the predictability of the hydrodynamic model. Indeed, the simulated recirculation flow patterns in the channel are significantly sensitive to the $k_{S\ Wall}$ parameter. As shown by Patzwahl and Güngör (2015) [6], this parameter could include several processes and physical configurations of the study site that are not represented explicitly in the model. As these elements vary depending on the water level, it is difficult to estimate the robustness of the numerical model in other discharge conditions. Furthermore, for high magnitude flood discharge values, the hydrodynamic feature of the study site may include flooded zones that are not represented in this work. In order to quantify and validate the robustness of this work, it could be interesting to perform other velocity measurements in the channel, for several discharge conditions.

The second point is about the bed load dynamic in the Loire River. This study has focused in great detail on the suspended sediment dynamics in one given configuration of the river bed. However, the bathymetry measurements have shown the presence of very mobile dunes on the Loire river bed. This observation is a sign of active bed load transport, even in case of moderate flood discharge conditions. This active bed load dynamic could greatly modify the bed configuration, and especially the position of alternate bars. Several studies ([2], [7], [5]) tried to estimate numerically or by field measurement this bar mobility, especially on the Loire River. This mobility could be accelerated or stopped by different anthropic or non-anthropic elements of the river bed, like a step for example. In this case, it could be interesting to know if the alternate bars configuration is stable (for example because of the step downstream the study site), or if it is dynamic with temporal cycles.

VI. Conclusion

In this study, a focus has been done on the suspended sediment dynamic in the Loire River. On a local river reach with an adjacent channel, a field campaign has shown that the flow velocities in the channel are strongly correlated to the discharge conditions in Loire River, and are structured with complex recirculation patterns. A TELEMAC 3D model has been calibrated to reproduce the measured velocities, with a good agreement. In order to reproduce the complex flow patterns in the channel, a specific value of $k_{S\ Wall}$ has been defined. Based on this calibration, three discharge scenarios and ten sediment classes have been simulated. The results show that the deposits observed in the adjacent channel are related to different upstream scenarios: the finer sediment classes ($D < 100$ μm) are transferred and deposited in the channel during low discharge conditions. During larger floods events with high suspended sediment concentrations, coarser sediment classes are deposited ($100 < D < 400$ μm) after being eroded from the sand river bed. This finding will be useful for river management, as well as for industrial activities. As a perspective, interesting work could be done in the future by using a multiclass sediment module in TELEMAC 3D.

REFERENCES

[1] B. Camenen, R. C. Grabowski, A. Latapie, A. Paquier, L. Solari, and S. Rodrigues, "On the estimation of the bed-material transport and budget along a river segment: application to the middle loire river, france," *Aquatic Sciences*, vol. 78, no. 1, pp. 71–81, 2016. [Online]. Available: http://dx.doi.org/10.1007/s00027-015-0442-3

[2] N. Claude, S. Rodrigues, V. Bustillo, J.-G. Brhret, P. Tassi, and P. Jug, "Interactions between flow structure and morphodynamic of bars in a channel expansion/contraction, loire river, france," *Water Resources Research*, vol. 50, no. 4, pp. 2850–2873, 2014. [Online]. Available: http://dx.doi.org/10.1002/2013WR015182

[3] J.-M. Hervouet, *Hydrodynamics of Free Surface Flows modelling with the finite element method.* Wiley, 2007.

[4] M. Jodeau and G. Antoine, "Telemac 3d and sediment transport : theoritical description - version 7.0. edf report." EDF R&D - LNHE, Tech. Rep., 2015.

[5] F. Mattia, D. Wang, J.-M. Hervouet, A. Leopardi, K. El kadi Abderrezzak, and P. Tassi, "Numerical simulations of bar formation and propagation in straight and curved channels," in *20th Telemac & Mascaret User Club*, 2013.

[6] R. Patzwahl and T. Güngör, "Horizontal flow field modelling in a channel mouth," in *22nd Telemac & Mascaret User Club*, 2015.

[7] S. Rodrigues, E. Mosselman, N. Claude, C. L. Wintenberger, and P. Juge, "Alternate bars in a sandy gravel bed river: generation, migration and interactions with superimposed dunes," *Earth Surface Processes and Landforms*, vol. 40, no. 5, pp. 610–628, 2015, eSP-13-0173.R2. [Online]. Available: http://dx.doi.org/10.1002/esp.3657

[8] J. Zyserman and J. Fredsoe, "Data analysis of bed concentration of suspended sediment," *Journal of Hydraulic Engineering*, vol. 120, no. 9, pp. 1021–1042, 1994.